Vol 11 No 11, November 2002
1009-1963/2002/11(11)/1115-09

Chinese Physics

© 2002 Chin. Phys. Soc.
and IOP Publishing Ltd

Study of the Wada fractal boundary and indeterminate crisis*

Hong Ling(洪 灵) and Xu Jian-Xue(徐健学)

Institute of Nonlinear Dynamics, Xi'an Jiaotong University, Xi'an 710049, China

(Received 30 December 2001; revised manuscript received 26 April 2002)

By using the generalized cell mapping digraph (GCMD) method, we study bifurcations governing the escape of periodically forced oscillators in a potential well, in which a chaotic saddle plays an extremely important role. In this paper, we find the chaotic saddle, and we demonstrate that the chaotic saddle is embedded in a strange fractal boundary which has the Wada property, that any point on the boundary of that basin is also simultaneously on the boundary of at least two other basins. The chaotic saddle in the Wada fractal boundary, by colliding with a chaotic attractor, leads to a chaotic boundary crisis with a global indeterminate outcome which presents an extreme form of indeterminacy in a dynamical system. We also investigate the origin and evolution of the chaotic saddle in the Wada fractal boundary, particularly concentrating on its discontinuous bifurcations (metamorphoses). We demonstrate that the chaotic saddle in the Wada fractal boundary is created by the collision between two chaotic saddles in different fractal boundaries. After a final escape bifurcation, there only exists the attractor at infinity; a chaotic saddle with a beautiful pattern is left behind in phase space.

Keywords: global analysis, generalized cell mapping, indeterminate chaotic boundary crisis, chaotic saddle, Wada fractal boundary

PACC: 0545

1. Introduction

Bifurcations of dynamical chaotic invariant sets, namely, how qualitative changes of the invariant sets occur as a system parameter changes, have been a central and important issue in the study of chaotic systems. It is known that there are commonly two types of dynamical chaotic invariant sets that occur in situations of physical interest, namely, chaotic attractors and chaotic saddles. Chaotic saddles are non-attracting dynamical invariant sets that can lead to a variety of physical phenomena, such as chaotic scattering and fractal basin boundaries.[1,2] Just as chaotic attractors can undergo discontinuous bifurcations (crises),[3,4] so can chaotic saddles. The discontinuous bifurcations (metamorphoses) of chaotic saddles result in physically observable phenomena, such as the enhancement of chaotic scattering[5] and basin boundary metamorphoses.[6−8] More recently, a type of fractal boundary having the Wada property—that every point on the common boundary of that basin and another basin is also on the boundary of a third basin, namely for basins $B(1), B(2), \cdots, B(N)$ $(N \geq 3)$ to satisfy $\overline{B}(1) = \overline{B}(2) = \cdots = \overline{B}(N)$ ($\overline{B}$ is the boundary of basin B)—has been identified in dynamical systems and studied.[9−11]

In the case of dissipative dynamical systems, we are usually interested in the asymptotic behaviour, in particular, in what can be observed after the transient disappears. For this reason, most studies of chaotic dynamics have concentrated on chaotic attractors, their bifurcations and fractal basin boundaries. In this paper, we have chosen to study the canonical escape equation, which was introduced by Thompson and co-workers[12−14] to model the most typical escape from a potential well. By means of the generalized cell mapping digraph (GCMD) method, we confirm previously reported results. In addition, we find a chaotic saddle and demonstrate that the chaotic saddle is embedded in a strange fractal boundary which has the Wada property, that any point on the boundary of that basin is also simultaneously on the boundary of at least two other basins. The chaotic saddle in the Wada fractal boundary plays an extremely important

*Project supported by the National Natural Science Foundation of China (Grant Nos 10172067 and 19972051).

role in the bifurcations governing escape. The chaotic saddle in the Wada fractal boundary, by colliding with a chaotic attractor, leads to a chaotic boundary crisis with a global indeterminate outcome, which presents an extreme form of indeterminacy in a dynamical system. We also investigate the origin and evolution of the chaotic saddle in the Wada fractal boundary, particularly concentrating on its discontinuous bifurcations (metamorphoses). We demonstrate that the chaotic saddle in the Wada fractal boundary is created by the collision between two chaotic saddles in different fractal boundaries. After a final escape bifurcation, there only exists the attractor at infinity; a chaotic saddle with a beautiful pattern is left behind in the phase space.

In the early 1980s, a generalized cell mapping (GCM) method for the global analysis of nonlinear systems was first introduced by Hsu.[15] Later, certain new developments of the GCM method were reported. Hsu[16] presented a theory of the subdomain-to-subdomain global transient analysis in 1992, and in 1995 Hsu[17] developed a generalized cell mapping method using posets and digraphs. More recently, Xu and Hong[18] further theoretically studied the correspondence between generalized cell mapping systems and digraphs directly in the cell state space. Hong and Xu[19] presented a generalized cell mapping digraph (GCMD) method on the basis of a correspondence between generalized cell mapping systems and digraphs, and this correspondence has been theoretically proven on the basis of set theory in the cell state space. The GCMD method is a new method to efficiently perform global analysis of nonlinear systems including global transient analysis by using digraphic algorithms on the basis of a strictly theoretical correspondence between generalized cell mapping systems and digraphs. The principal advantages of the GCMD method[18−23] are as follows: (1) it can determine unstable (non-attracting) invariant sets in phase space including unstable (non-attracting) chaotic invariant sets; (2) it gives us a picture of the global transient evolution process by using topological sorting algorithms; (3) only Boolean operations (namely the logical operations of variables 0 and 1) are adopted in the analysis of global qualitative properties. As a result, the multifaceted complex behaviour of nonlinear systems can be efficiently studied in a new way.

The organization of this paper is as follows. In section 2 the single-domicile transient sets corresponding to basins of attraction and the multiple-domicile transient sets corresponding to boundaries of basins are discussed. In section 3 we briefly introduce Thompson's escape equation, including an optimal escape route of interest. In section 4 we apply the GCMD method to investigate the bifurcations governing escape along the optimal escape route. Some final conclusions are given in section 5.

2. Single-domicile transient sets and multiple-domicile transient sets

From the definition of the domicile of a transient cell,[15,18,19] if a transient cell j leads to a persistent self-cycling set $P(i)$, then we call $P(i)$ a domicile of cell j. A transient cell can have several domiciles. Transient cells may be classified according to the number of domiciles they have. In particular, transient cells which have only one domicile are called single-domicile transient cells, and those which have more than one are called multiple-domicile transient cells. The single-domicile transient cells form basins of attraction, and the multiple-domicile transient cells form the boundaries separating the basins of attraction.

The domiciles of the transient cells provide a very natural way of partitioning the transient cells into transient sets. Let there be N_p persistent self-cycling sets which are denoted by $P(i)$, i=1, 2,..., N_p. The set consisting of all the single-domicile transient cells having the ith persistent self-cycling set as its domicile is called the ith single-domicile transient set and is denoted by $B(i)$ where i=1, 2,..., N_p. It populates the domain of attraction of the ith persistent self-cycling set.

The set consisting of all the multiple-domicile transient cells, having ith and jth persistent self-cycling sets as their only domiciles, is called the (i,j)th two-domicile transient set and is denoted by $B(i,j)$ where i, j =1, 2,..., N_p, and $i \neq j$. The region populated by this set $B(i,j)$ is the boundary between the ith and jth domains of attraction $B(i)$, $B(j)$. There are altogether $C^2_{N_p}$ two-domicile transient sets, where $C^2_{N_p}$ is the binomial coefficient $N_p(N_p-1)/2$.

The set consisting of all the multiple-domicile transient cells, having ith, jth and kth persistent self-cycling sets as their only domiciles, is called the (i,j,k)th three-domicile transient set and is denoted by $B(i,j,k)$ where i, j, k=1, 2,..., N_p, and $i \neq j \neq k$. The region populated by this set is the boundary

between the ith, jth and kth domains of attraction $B(i), B(j), B(k)$. There are altogether $C^3_{N_p}$ three-domicile transient sets, where $C^3_{N_p}$ is the binomial coefficient $N_p(N_p-1)(N_p-2)/6$. In terms of this partitioning of the transient cells, the transient sets with four or more domiciles are defined in a similar way. The final one of the sequence is a single N_p-domicile transient set, in which each cell has its trajectories going to all the persistent self-cycling sets $P(i)$, i=1, 2,..., N_p. In total, there are $2^{N_p}-1$ transient sets besides the N_p persistent self-cycling sets.

3. Thompson's escape equation and an optimal escape route

The canonical escape equation describing the sinusoidally forced motions of a particle in a potential $V(x) = x^2/2 - x^3/3$ with inertia and linear viscous damping ($\beta > 0$) is given by Thompson and Soliman:[12]

$$\frac{\mathrm{d}^2x}{\mathrm{d}t^2} + \beta\frac{\mathrm{d}x}{\mathrm{d}t} + x - x^2 = F\sin(\omega t + \phi). \qquad (1)$$

Here the damping coefficient β, forcing magnitude F and forcing frequency ω are treated as system parameters. Thompson has studied the forced oscillator (1) in considerable detail for the case of β=0.1, and has given a bifurcation diagram in the (ω, F) control space, as shown in Figure 1 of Ref.[12]. Here we are primarily interested in the region around the optimal escape at Q, where the system can escape at a minimum forcing magnitude F. The bifurcation diagram near the optimal escape is reproduced here as Fig.1. As shown in Fig.1, there are six bifurcation curves, namely, the two saddle-node fold curves A and B, the dashed flip curve C for the period doubling cascade, the boundary crisis curve E, the homoclinic tangency curve M, and the heteroclinic tangency curve H. Two coexisting attractors within the well are found in the triangular region bounded by curves A, B and E. The shaded region in Fig.1 defines parameter values for which all motions must escape to infinity. In this paper, we choose a vertical escape route ω=0.827 that is very close to the optimal escape Q, and is at the left of Q ($\omega < \omega^Q$). By means of GCMD method, we confirm the previously reported results, and in addition, we find a chaotic saddle, and show that the chaotic saddle is embedded in a Wada fractal boundary. The chaotic saddle in the Wada fractal boundary plays an extremely important role in the bifurcations governing escape. We also investigate the origin and evolution of the chaotic saddle in the Wada fractal boundary, particularly concentrating on its discontinuous bifurcations (metamorphoses).

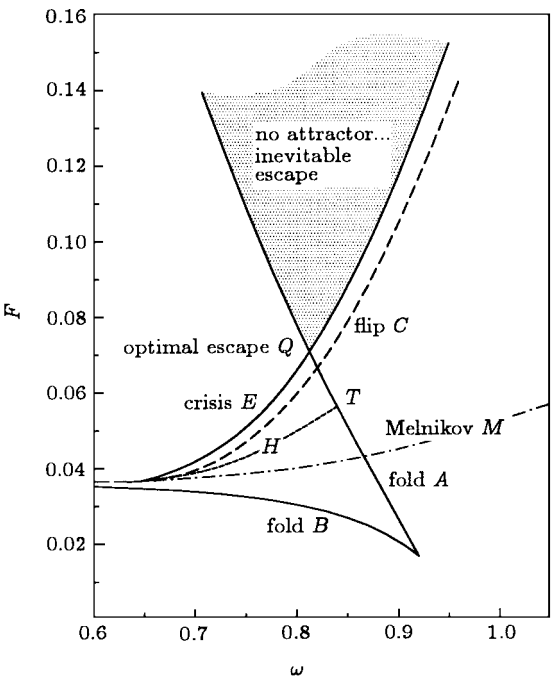

Fig.1. For the escape equation (1) with β=0.1, $\phi = 180°$, bifurcation diagram in the (ω, F) control space near the optimal escape. Escape from the potential well is inevitable in the shaded region.

4. The bifurcations governing escape along an optimal escape route

In this section, we apply the GCMD method to investigate the bifurcations governing escape along an optimal escape route ω=0.827. There are three main bifurcations besides the saddle-node bifurcation crossing the fold curve B. The first bifurcation, crossing the heteroclinic tangency curve H, is the bifurcation in the F interval (0.0705, 0.071) that creates a chaotic saddle in a Wada fractal boundary. The second bifurcation, crossing the crisis curve E by increasing the forcing magnitude F, is an indeterminate chaotic boundary crisis in the F interval (0.081, 0.0815). The third bifurcation, crossing the fold curve A by further increasing F, is a saddle-node fold bifurcation in the F interval (0.0815, 0.082).

In the applying GCMD method, a grid structure of 105×105 cells is used for the region of the state space $(-0.8 \le x \le 1.2)\times(-0.9 \le \mathrm{d}x/\mathrm{d}t \le 0.8)$, therefore the cell size is 0.01905×0.01619, and 25×25 interior sampling points are used within each cell. Thus, there are a total of 105×105+1 regular cells, plus a sink cell which covers the state space outside the region of interest.

In the case of F=0.04, below the fold curve B, we find one persistent self-cycling set and one transient self-cycling set. The acyclic (namely the period of a self-cycling set is one) persistent self-cycling set corresponds to a period-1 attractor, namely, non-resonant attractor S_{n} (marked by the symbol "●"), the acyclic transient self-cycling set having only one cell corresponds to a period-1 saddle on the basin boundary, namely the hilltop saddle D_{h} (marked by the symbol "◇"). The above correspondences are further confirmed by the refining process of self-cycling sets, that is, under iterative refinement, the region occupied by the persistent and the transient self-cycling sets becomes smaller and smaller, approaching a point in the limit. In this case, the total number of persistent self-cycling sets (attractors), including a sink cell which is the attractor at infinity, is equal to two. And here, the sink cell and the non-resonant attractor S_{n} are respectively denoted by $P(1)$, $P(2)$ in sequence. Thus, the domain of attraction $B(1)$ of the attractor $P(1)$ is marked by the symbol "·", and the domain of attraction $B(2)$ of the attractor $P(2)$ is marked by the symbol "×". For this case there are two attractors, then there is one two-domicile transient set $B(1,\ 2)$. The two-domicile transient set $B(1,\ 2)$, namely, the boundary between the domains of attraction of the attractors $P(1)$ and $P(2)$, is marked by the symbol "1". The above results are shown in Fig.2(a).

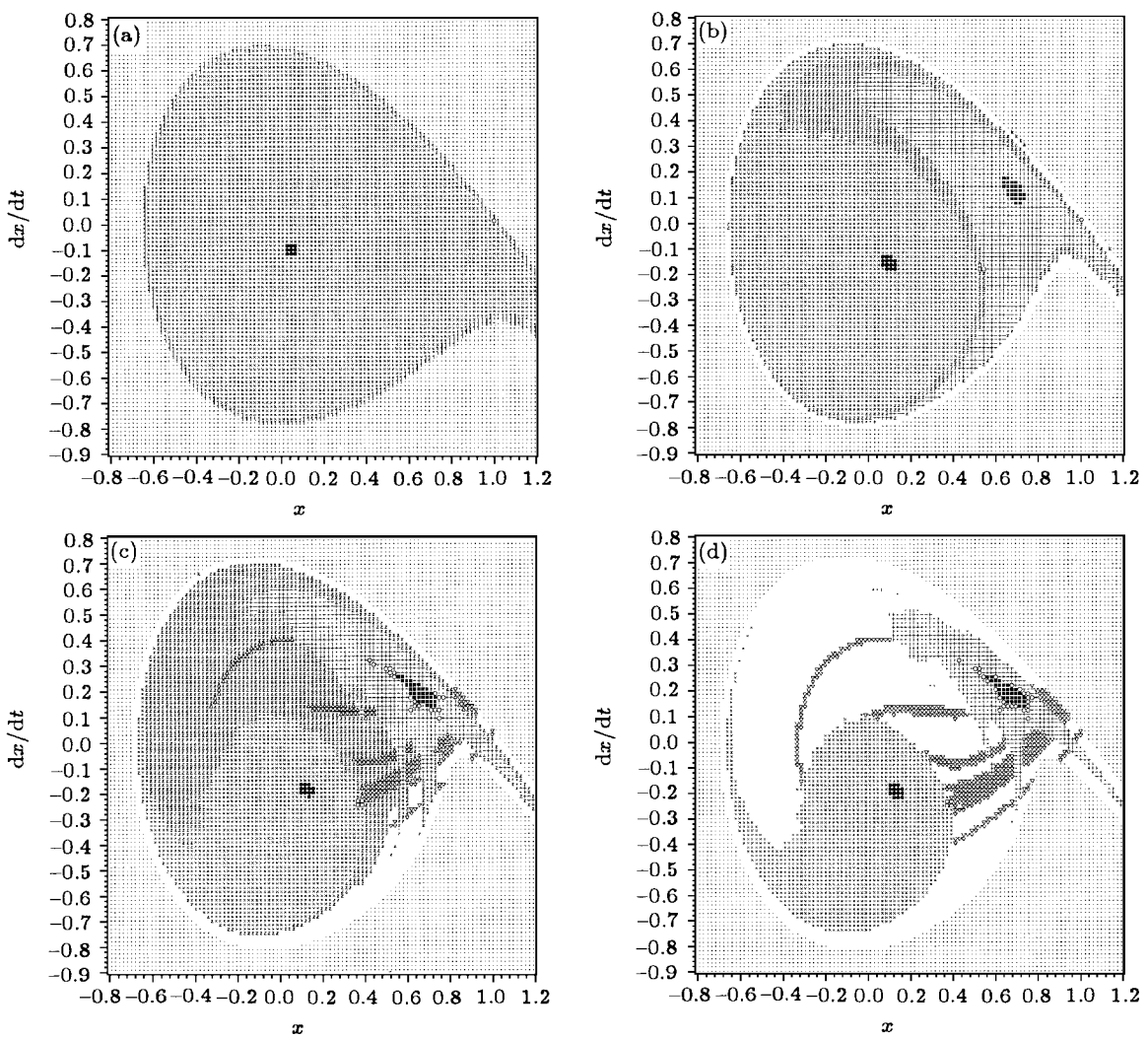

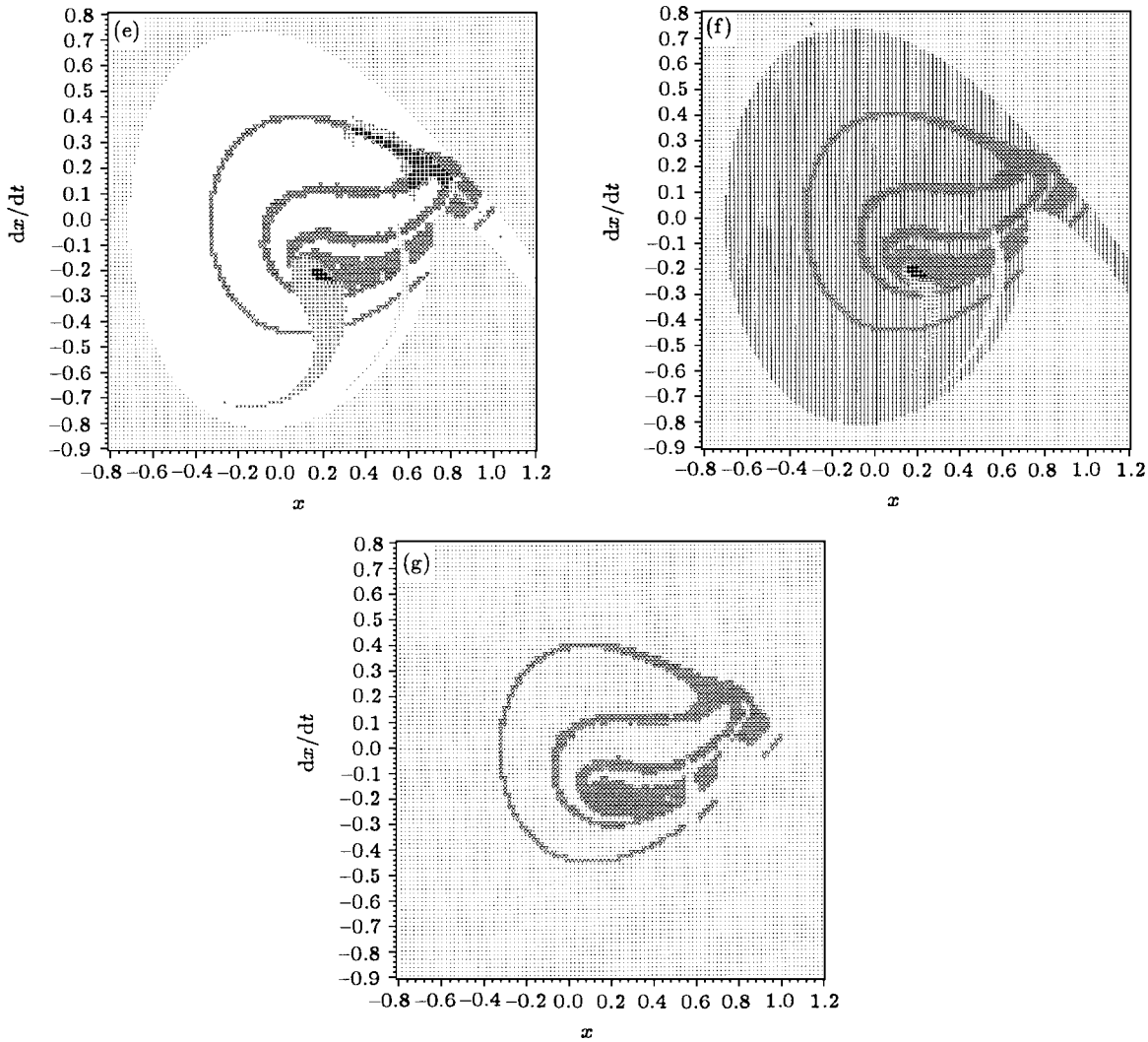

Fig.2. For the escape equation (1) with β=0.1, $\phi = 180°$, three main bifurcations along the optimal escape route ω=0.827. The attractor $P(2)$ is marked by the symbol "●". The attractor $P(3)$ is marked by the symbol "■". The hilltop saddle D_h is marked by the symbol "◇". The resonant saddle D_r is marked by the symbol "□". The chaotic saddle is marked by the symbol "∇", and the chaotic saddle in the boundary $B(2, 3)$ is marked by the symbol "Δ". A transient process is marked by the symbol "○". The domain of attraction $B(1)$ of the sink cell $P(1)$ is marked by the symbol "·", the domain of attraction $B(2)$ of the attractor $P(2)$ is marked by the symbol "×", and the domain of attraction $B(3)$ of the attractor $P(3)$ is marked by the symbol "+". The boundary $B(1, 2)$ is marked by the symbol "1". The boundary $B(1, 3)$ is marked by the symbol "k", the boundary $B(2, 3)$ is marked by the symbol "z", and the boundary $B(1, 2, 3)$ is marked by the blank space. (a) F=0.04; (b) F=0.06; (c) F=0.0705; (d) F=0.071; (e) F=0.081; (f) F=0.0815; (g) F=0.082.

In the case of F=0.06, above the fold curve B, we find two persistent self-cycling sets and two transient self-cycling sets. The two acyclic persistent self-cycling sets (under iterative refinement approaching a point in the limit) correspond to two period-1 attractors, namely, the non-resonant attractor S_n and the resonant attractor S_r. The attractor S_n is marked by the symbol "●" and the attractor Sr is marked by the symbol "■". The two acyclic transient self-cycling sets (under iterative refinement approaching a point in the limit) correspond to two period-1 saddles on different basin boundaries, namely, the hilltop saddle D_h and the resonant saddle D_r. The saddles D_h and D_r are marked respectively by the symbols "◇" and "□". In this case, the total number of persistent self-cycling sets (attractors), including a sink cell, is equal to three. And here, the sink cell, the non-resonant attractor S_n and the resonant attractor S_r are respectively denoted by $P(1)$, $P(2)$, $P(3)$ in sequence (which is used throughout this paper). Thus, the domain of attraction $B(1)$ of the attractor $P(1)$ is marked by the symbol "·", the domain of attraction

$B(2)$ of the attractor $P(2)$ is marked by the symbol "×", and the domain of attraction $B(3)$ of the attractor $P(3)$ is marked by the symbol "+". For this case there are three attractors, then there are three two-domicile transient sets $B(1, 2)$, $B(1, 3)$ and $B(2, 3)$, and one three-domicile transient set $B(1, 2, 3)$. The two-domicile transient set $B(1, 2)$, namely the boundary between the domains of attraction of the attractors $P(1)$ and $P(2)$, is an empty set. The two-domicile transient set $B(1, 3)$, namely the boundary between the domains of attraction of the attractors $P(1)$ and $P(3)$, is marked by the symbol "k". The two-domicile transient set $B(2, 3)$, namely the boundary between the domains of attraction of the attractors $P(2)$ and $P(3)$, is marked by the symbol "z". The three-domicile transient set $B(1, 2, 3)$, namely the boundary between the domains of attraction of the attractors $P(1)$, $P(2)$ and $P(3)$, is marked by the blank space. In particular, it should be noted that the saddle $D_{\rm r}$ is in the boundary $B(2, 3)$, and the saddle $D_{\rm h}$ is in the boundary $B(1, 2, 3)$. The above results are shown in Fig.2(b). (Note that the symbols are used throughout this paper.)

4.1. The bifurcation that creates a chaotic saddle in a Wada fractal boundary in the F interval (0.0705, 0.071)

The first bifurcation that creates a chaotic saddle in a Wada fractal boundary in the F interval (0.0705, 0.071) is shown in Figs.2(c) and (d).

In the case F=0.0705, we find two persistent self-cycling sets and four transient self-cycling sets. The two acyclic persistent self-cycling sets (under iterative refinement approaching a point in the limit) correspond respectively to two period-1 attractors $S_{\rm n}$ and $S_{\rm r}$. The attractor $S_{\rm n}$ is marked by the symbol "●" and the attractor $S_{\rm r}$ is marked by the symbol "■". The two acyclic transient self-cycling sets (under iterative refinement disclosing more and more of their fine structure without major changes in their overall size of occupation in the state space) correspond respectively to two chaotic saddles; one is marked by the symbol "∇" and the other is marked by the symbol "Δ". The third acyclic transient self-cycling set having only four cells (under iterative refinement approaching a point in the limit) corresponds to a period-1 saddle $D_{\rm r}$ (marked by the symbol "□"). The fourth transient self-cycling set (under iterative refinement disappearing) does not correspond to any unstable solution, namely, it is a transient process (marked by the symbol "○"). For this case there are three attractors including a sink cell, namely $P(1)$, $P(2)$ and $P(3)$, three single-domicile transient sets $B(1)$, $B(2)$ and $B(3)$, three two-domicile transient sets $B(1, 2)$, $B(1, 3)$ and $B(2, 3)$, and one three-domicile transient set $B(1, 2, 3)$. The boundary $B(1, 2)$ is an empty set, the boundary $B(1, 3)$ having only one cell is marked by the symbol "k", the boundary $B(2, 3)$ is a fractal boundary marked by the symbol "z", and the boundary $B(1, 2, 3)$ is a fractal boundary marked by the blank space. The fractal boundaries $B(2, 3)$ and $B(1, 2, 3)$ are further confirmed by the boundary refinement method introduced in Ref.[14]. In particular, it should be noted that the chaotic saddle marked by the symbol "∇" is in the fractal boundary $B(1, 2, 3)$, the chaotic saddle marked by the symbol "Δ" is in the fractal boundary $B(2, 3)$, and the saddle $D_{\rm r}$ is on the edge of the basin interior $B(2)$. Fig.2(c) shows that the two chaotic saddles are touching each other.

In the case F=0.071, we find two persistent self-cycling sets and three transient self-cycling sets. The two acyclic persistent self-cycling sets correspond to two period-1 attractors $S_{\rm n}$ and $S_{\rm r}$. The attractor $S_{\rm n}$ is marked by the symbol "●" and the attractor Sr is marked by the symbol "■". The huge acyclic transient self-cycling set corresponds to a chaotic saddle (marked by the symbol "∇"). The second acyclic transient self-cycling set having only four cells corresponds to a period-1 saddle $D_{\rm r}$ (marked by the symbol "□"). The third transient self-cycling set does not correspond to any unstable solution; it is a transient process (marked by the symbol "○"). The above correspondences are further confirmed by the refining process of self-cycling sets. For this case, there are three attractors including a sink cell, namely $P(1)$, $P(2)$ and $P(3)$, three single-domicile transient sets $B(1)$, $B(2)$ and $B(3)$, three two-domicile transient sets $B(1, 2)$, $B(1, 3)$ and $B(2, 3)$, and one three-domicile transient set $B(1, 2, 3)$. In this case, all the two-domicile transient sets $B(1, 2)$, $B(1, 3)$ and $B(2, 3)$ are empty sets, the boundary $B(1, 2, 3)$ is marked by the blank space, as shown in Fig.2(d), the thickness of the boundary $B(1, 2, 3)$ is far larger than the maximum of the cell sizes in all the coordinate directions, and the boundary $B(1, 2, 3)$ is a fractal boundary and can also be further confirmed by the boundary refinement method. In particular, the fractal boundary $B(1, 2, 3)$ has the Wada property that every point on the common boundary of that basin and another basin

is also on the boundary of a third basin, i.e. the condition $\overline{B}(1) = \overline{B}(2) = \overline{B}(3) = B(1,2,3)$ is satisfied, where $\overline{B}(i)$ is the boundary of the basin $B(i)$. Also, the chaotic saddle is embedded in the Wada fractal boundary $B(1, 2, 3)$.

Figures 2(c) and (d) show that the chaotic saddle in the Wada fractal boundary is created by the collision between the two chaotic saddles in different fractal boundaries.

The illustration of Figs.2(c) and (d) is given as follows. In Fig.2(c), the stable manifold of the chaotic saddle marked by the symbol "∇" is the boundary $B(1, 2, 3)$. Its unstable manifold has three unstable branches which extend respectively toward three attractors $P(1)$, $P(2)$ and $P(3)$. Similarly, the stable manifold of the chaotic saddle marked by the symbol "Δ" is the boundary $B(2, 3)$. Its unstable manifold has two unstable branches which extend respectively toward two attractors $P(2)$ and $P(3)$. Due to the collision between the two chaotic saddles, the points of the boundary $B(2, 3)$ are attracted to the chaotic saddle marked by the symbol "Δ", and then can be sent to the attractor $P(1)$ along the unstable manifold of the chaotic saddle marked by the symbol "∇".

4.2. The indeterminate chaotic boundary crisis in the F interval (0.081, 0.0815)

The indeterminate chaotic boundary crisis in the F interval (0.081, 0.0815) is shown in Figs.2(e) and (f).

In the case F=0.081, we find two persistent self-cycling sets and two transient self-cycling sets. The two acyclic persistent self-cycling sets correspond respectively to a period-1 attractor $S_{\rm n}$ (marked by the symbol "$\bullet$") and a chaotic attractor (marked by the symbol "$\blacksquare$"). The two acyclic transient self-cycling sets correspond respectively to a period-1 saddle $D_{\rm r}$ (marked by the symbol "$\square$") and a chaotic saddle (marked by the symbol "∇"). The above correspondences are further confirmed by the refining process of self-cycling sets. For this case, there are three attractors including a sink cell, namely $P(1)$, $P(2)$ and $P(3)$, three single-domicile transient sets $B(1)$, $B(2)$ and $B(3)$, three two-domicile transient sets $B(1, 2)$, $B(1, 3)$ and $B(2, 3)$, and one three-domicile transient set $B(1, 2, 3)$. In this case, all the two-domicile transient sets $B(1, 2)$, $B(1, 3)$ and $B(2, 3)$ are empty sets. The boundary $B(1, 2, 3)$ is marked by the blank space, as shown in Fig.2(e). The thickness of the boundary $B(1, 2, 3)$ is far larger than the maximum of the cell sizes in all the coordinate directions. The boundary $B(1, 2, 3)$ is a fractal boundary, and can also be further confirmed by the boundary refinement method. In particular, the fractal boundary $B(1, 2, 3)$ has the Wada property that every point on the common boundary of that basin and another basin is also on the boundary of a third basin, and the chaotic saddle is embedded in the Wada fractal boundary $B(1, 2, 3)$. Fig.2(e) shows that the chaotic attractor is touching the chaotic saddle in the Wada fractal boundary $B(1, 2, 3)$.

In the case F=0.0815, we find only one persistent self-cycling set and two transient self-cycling sets. The acyclic persistent self-cycling set corresponds to a period-1 attractor $S_{\rm n}$ (marked by the symbol "$\bullet$"). The two acyclic transient self-cycling sets correspond respectively to a period-1 saddle $D_{\rm r}$ (marked by the symbol "$\square$") and a chaotic saddle (marked by the symbol "∇"). The above correspondences are further confirmed by the refining process of self-cycling sets. For this case, there are two attractors including a sink cell, namely $P(1)$ and $P(2)$, two single-domicile transient sets $B(1)$ and $B(2)$, one two-domicile transient set $B(1, 2)$. The boundary $B(1, 2)$ is marked by the symbol "1", as shown in Fig.2(f). The thickness of the boundary $B(1, 2)$ is far larger than the maximum of the cell sizes in all the coordinate directions. The boundary $B(1, 2)$ is a fractal boundary, and can also be further confirmed by the boundary refinement method. In particular, the chaotic saddle is embedded in the fractal boundary $B(1, 2)$.

Figures 2(e) and (f) show that the indeterminate chaotic boundary crisis in the F interval (0.081, 0.0815) is caused by the collision between the chaotic attractor and the chaotic saddle in the Wada fractal boundary. In such a case, the chaotic attractor and its basin of attraction are suddenly destroyed. The chaotic saddle also undergoes an abrupt enlargement in its size, i.e. the chaotic attractor is converted into a new incremental portion of the chaotic saddle after the collision, and simultaneously the Wada fractal boundary $B(1, 2, 3)$ disappears after the collision, i.e. it is converted into the fractal boundary $B(1, 2)$ between the basins of attraction of two remaining attractors $P(1)$ and $P(2)$ (Wada-fractal boundary bifurcation). In particular, the chaotic saddle after the crisis is in the fractal boundary $B(1, 2)$. This implies that the outcome of the chaotic boundary crisis is indeterminate, i.e. after the system drifts through the crisis,

which of the two remaining attractors the orbit goes to is indeterminate in that it is sensitively dependent on arbitrarily small effects such as how the parameter is changed and/or noise and/or computer roundoff. Obviously, this presents an extreme form of indeterminacy in a dynamical system.

The illustration of Figs.2(e) and (f) is given as follows. In Fig.2(e), the stable manifold of the chaotic saddle is the boundary $B(1, 2, 3)$; that is, points on the boundary $B(1, 2, 3)$ are attracted to the chaotic saddle, and three unstable branches of its unstable manifold, along which points are repelled from the chaotic saddle, are directed respectively to three attractors $P(1)$, $P(2)$ and $P(3)$. We see from Fig.2(e) that part (the closure) of the unstable manifold, namely, the chaotic attractor $P(3)$, actually touches the stable manifold, the basin boundary $B(1, 2, 3)$, in several places at the same time, i.e. homoclinic tangency occurs. Hence the points of the region $B(3)$ and $P(3)$ will eventually touch the chaotic saddle, and then be sent to two remaining attractors $P(1)$ and $P(2)$ along the unstable manifold of the chaotic saddle. We also see from Fig.2(f) that the chaotic saddle after the chaotic boundary crisis is embedded in the fractal boundary $B(1, 2)$ of the two remaining attractors $P(1)$ and $P(2)$. As a result, which of the two remaining attractors $P(1)$ and $P(2)$ the points go to is indeterminate. This is the most complete illustration of the indeterminate chaotic boundary crisis.

4.3. The saddle-node fold bifurcation in the F interval (0.0815, 0.082)

The saddle-node fold bifurcation in the F interval (0.0815, 0.082) is shown in Figs.2(f) and (g).

In the case F=0.082, we find only one transient self-cycling set. The huge acyclic transient self-cycling set corresponds to a chaotic saddle (marked by the symbol "∇"). In this case, there is only one attractor $P(1)$. The basin of attraction $B(1)$ of the attractor $P(1)$ is marked by the symbol ".", and the chaotic saddle is in the basin interior $B(1)$.

Figures 2(f) and (g) show that at the saddle-node fold bifurcation the saddle of the saddle-node fold is located in tangency with the chaotic saddle in the fractal boundary $B(1, 2)$ of the two attractors $P(1)$ and $P(2)$. The attractor (node) and the saddle are merged into the chaotic saddle and the chaotic saddle also undergoes an abrupt enlargement in size. Simultaneously the fractal boundary $B(1, 2)$ disappears, i.e. a fractal-smooth boundary bifurcation occurs.

4.4. The dimension of a Wada fractal boundary

The dimension of a fractal basin boundary can be numerically calculated on the basis of the theory of the uncertainty exponent.[1] The uncertain fraction $f(\varepsilon)$ of a finite region of a D-dimensional phase space associated with initial condition error ε obeys

$$f(\varepsilon) \sim \varepsilon^{\alpha}, \tag{2}$$

$$d = D - \alpha, \tag{3}$$

where D is the phase space dimensionality, d is box-counting dimension of the basin boundary, and α is the uncertainty exponent. For a nonfractal basin boundary $\alpha = 1$; for a fractal basin boundary $\alpha < 1$.

We proceed as follows. Setting the initial condition error ε equal to the cell size, the uncertain fraction $f(\varepsilon)$ is the portion of the basin boundary in the region of interest. Hence, $f(\varepsilon)$ can be defined by

$$f(\varepsilon) = \frac{N(\varepsilon)}{N}, \tag{4}$$

where $N(\varepsilon)$ is the number of cells of the Wada boundary $B(1, 2, 3)$, and N is the totality of cells of the chosen region.

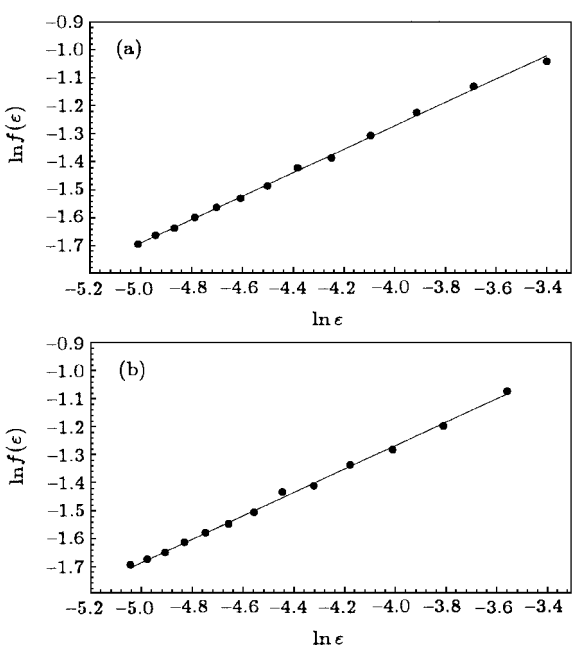

Fig.3. ln–ln plot of $f(\varepsilon)$ versus ε for the escape equation (1) with β=0.1, $\phi = 180°$, and F=0.073.

A square cell structure (grid) with the cell size (edge length) $\varepsilon = 1/(20+10i)$ (i=1, 2, $\cdots$, 13) is used in our computations. The ln–ln plot of $f(\varepsilon)$ versus ε is shown in Fig.3(a). The straight line fit indicates that $f(\varepsilon)$ scales as a power of ε, and the slope of the

line gives the power α. By using the least-squares estimation, the results are the uncertainty exponent α_1=0.414576, the mean square error e_1=8.310×10^{-3}.

Another cell structure with the cell size ε=1/(25+10 i) (i=1, 2, $\cdots$, 13) is chosen to give a good estimation for the significant figures of the dimension d. The ln–ln plot of $f(\varepsilon)$ versus ε is shown in Fig.3(b). The results are the uncertainty exponent α_2=0.4109122, the mean square error e_2=8.637×10^{-3}.

From α_1 and α_2, it can be obtained that the accuracy of the uncertainty exponent α is to two digits of decimals. Thus, the formula (3) yields the dimension $d \approx$1.59.

5. Conclusions

Using the GCMD method, we have studied bifurcations governing the escape of periodically forced oscillators along an optimal escape route. The main conclusions are as follows.

A chaotic saddle in a Wada fractal boundary is created by the collision between two chaotic saddles in different fractal boundaries.

An indeterminate chaotic boundary crisis is caused by the collision between a chaotic attractor and a chaotic saddle in a Wada fractal boundary. In such a case, the chaotic attractor and its basin of attraction are suddenly destroyed, and the chaotic saddle also undergoes an abrupt enlargement in size; that is, the chaotic attractor is converted into a new incremental portion of the chaotic saddle after the collision. Simultaneously, the Wada fractal boundary disappears after the collision, i.e. it is converted into the fractal boundary of two remaining attractors (Wada fractal boundary bifurcation). In particular, the chaotic saddle after the crisis is in the fractal boundary. This implies that the outcome of the chaotic boundary crisis is indeterminate, i.e. after the system drifts through the crisis, which of the two remaining attractors the orbit goes to is indeterminate in that it is sensitively dependent on arbitrarily small effects such as how the parameter is changed and/or noise and/or computer roundoff. Obviously, this presents an extreme form of indeterminacy in a dynamical system.

After a final escape bifurcation, there only exists the attractor at infinity; a chaotic saddle with a beautiful pattern is left behind in phase space.

References

[1] McDonald S W, Grebogi C, Ott E and Yorke J A 1985 *Physica* D **17** 125

[2] Ott E and Tél T 1993 *Chaos* **3** 417

[3] Grebogi C, Ott E and Yorke J A 1983 *Physica* D **7** 181

[4] Ma M Q, Wang W X and He D R 2000 *Acta Phys. Sin.* **49** 1679 (in Chinese)

[5] Lai Y C, Grebogi C, Blümel R and Kan I 1993 *Phys. Rev. Lett.* **71** 2212

[6] Grebogi C, Ott E and Yorke J A 1986 *Phys. Rev. Lett.* **56** 1011

[7] Grebogi C, Ott E and Yorke J A 1987 *Physica* D **24** 243

[8] Tan N, Xu J X and Chen Y H 2002 *Chin. Phys.* **11** 670

[9] Kennedy J and Yorke J A 1991 *Physica* D **51** 213

[10] Nusse H E and Yorke J A 1996 *Physica* D **90** 242

[11] Nusse H E, Ott E, Yorke J A 1995 *Phys. Rev. Lett.* **75** 2482

[12] Thompson J M T and Soliman M S 1991 *Proc. R. Soc.* A **432** 101

[13] Soliman M S and Thompson J M T 1992 *Phys. Rev.* A **45** 3425

[14] Gong P L, Xu J X and Sun Z C 2001 *Acta Phys. Sin.* **50** 841 (in Chinese)

[15] Hsu C S 1987 *Cell-to-Cell Mapping: A Method of Global Analysis for Nonlinear Systems* (New York: Springer-Verlag) pp 280–283

[16] Hsu C S 1992 *Int. J. Bifurcation Chaos* **2** 727

[17] Hsu C S 1995 *Int. J. Bifurcation Chaos* **5** 1085

[18] Xu J X and Hong L 1999 *Acta Mech. Sin.* **31** 724 (in Chinese)

[19] Hong L and Xu J X 1999 *Phys. Lett.* A **262** 361

[20] Hong L and Xu J X 2000 *Acta Phys. Sin.* **49** 1227 (in Chinese)

[21] Hong L and Xu J X 2001 *Acta Phys. Sin.* **50** 612 (in Chinese)

[22] Hong L and Xu J X 2001 *Int. J. Bifurcation Chaos* **11** 723

[23] Hong L and Xu J X 2001 *Acta Mech. Sin.* **33** 423 (in Chinese)